

Supplementary information for “Time and dose-dependent risk of pneumococcal pneumonia following influenza: A model for within-host interaction between influenza and *Streptococcus pneumoniae*”

Sourya Shrestha^{1,2,*}, Betsy Foxman⁴, Suzanne Dawid⁶, Allison E. Aiello^{4,5}, Brian M. Davis^{4,5}, Joshua Berus³ & Pejman Rohani^{1,2,7}

1 Department of Ecology & Evolutionary Biology, University of Michigan, Ann Arbor, MI 48109, USA

2 Center for the Study of Complex Systems, University of Michigan, Ann Arbor, MI 48109, USA

3 Undergraduate Research Opportunity Program, University of Michigan, Ann Arbor, MI 48109, USA

4 Department of Epidemiology, University of Michigan-School of Public Health, Ann Arbor, MI 48109, USA

5 Center for Social Epidemiology & Population, University of Michigan-School of Public Health, Ann Arbor, MI 48109, USA

6 Department of Pediatrics and Communicable Diseases, University of Michigan-School of Medicine, Ann Arbor, MI 48109, USA

7 Fogarty International Center, National Institutes of Health, Bethesda, MD 20892, USA

* E-mail: sourya@umich.edu

The influenza model.

We have adapted the empirically-motivated within-host model proposed by Handel *et al.* [1]. The state variables are defined as follows. V : viral titer; IR_A : adaptive immunity (antibodies); IR_I : innate immunity (type-I and type-II cytokines); E_U : uninfected epithelial cells; E_E : exposed cells; E_I : infectious virus-producing cells; E_D : dead cells. The system of delayed differential equations describing the model is given by:

$$\begin{aligned} \frac{dV}{dt} &= \frac{p E_I}{1 + \kappa IR_I(t - \tau_V)} - c V - \gamma b E_U V - k V IR_A \\ \frac{dIR_A}{dt} &= f V + r IR_A \\ \frac{dIR_I}{dt} &= p_1 V - p_2 IR_I \\ \frac{dE_U}{dt} &= \lambda E_D - b E_U V \\ \frac{dE_E}{dt} &= b E_U V - g E_E \\ \frac{dE_I}{dt} &= g E_E - d E_I \\ \frac{dE_D}{dt} &= d E_I - \lambda E_D \end{aligned} \quad (\text{S-1})$$

In table S-1, we provide the biological description and estimated values of model parameters. Please refer the original paper [1], for details on the estimates. The initial conditions used to solve the system are also taken from the original paper [1], where $V(0) = 4 \times 10^4$, $E_U(0) = 7 \times 10^9$, and the rest of the variables are initialized at 0. We emphasize that our model presented in equations (S-1) contains a modified term for the innate immune response (IR_I). Specifically, we have adopted a different functional form, whereby the innate immune response is stimulated by the viral load. The new parameters, p_1 and p_2 , are chosen to give dynamics (both viral and the innate immunity) consistent with empirical data presented in Handel *et al.* [1]. Further, as we confirm in Fig. S-2, our model generates qualitatively similar results.

Table S-1. Parameters and estimates for the Influenza model.

Parameter	Description	Estimate
$1/g$	duration of latent eclipse phase	0.25 days
$1/d$	lifespan of infected cells	0.5 days
$1/c$	lifespan of free virions	0.2 days
b	infection rate	1.9×10^{-7} PFU per day
p	virus production rate	1 PFU per day
λ	rate of regeneration of epithelial cells	1.5×10^{-2} cells per day
γ	conversion between infectious virions and PFU	1.3×10^{-1} virus:PFU
κ	strength of innate IR	4.5×10^{-2} units per day
r	expansion rate of adaptive IR	0.27 units per day
f	recruitment rate of adaptive IR	2.8×10^{-6} units per day
k	kill rate of adaptive IR	20 per day
m	growth/decay rate of innate IR	$1.24 t \leq 5; -1.17 t > 5$
τ_V	delay for innate IR	1.3 days
p_1	stimulation of IR_I	0.0005 day^{-1}
p_2	decay rate of IR_I	1 day^{-1}

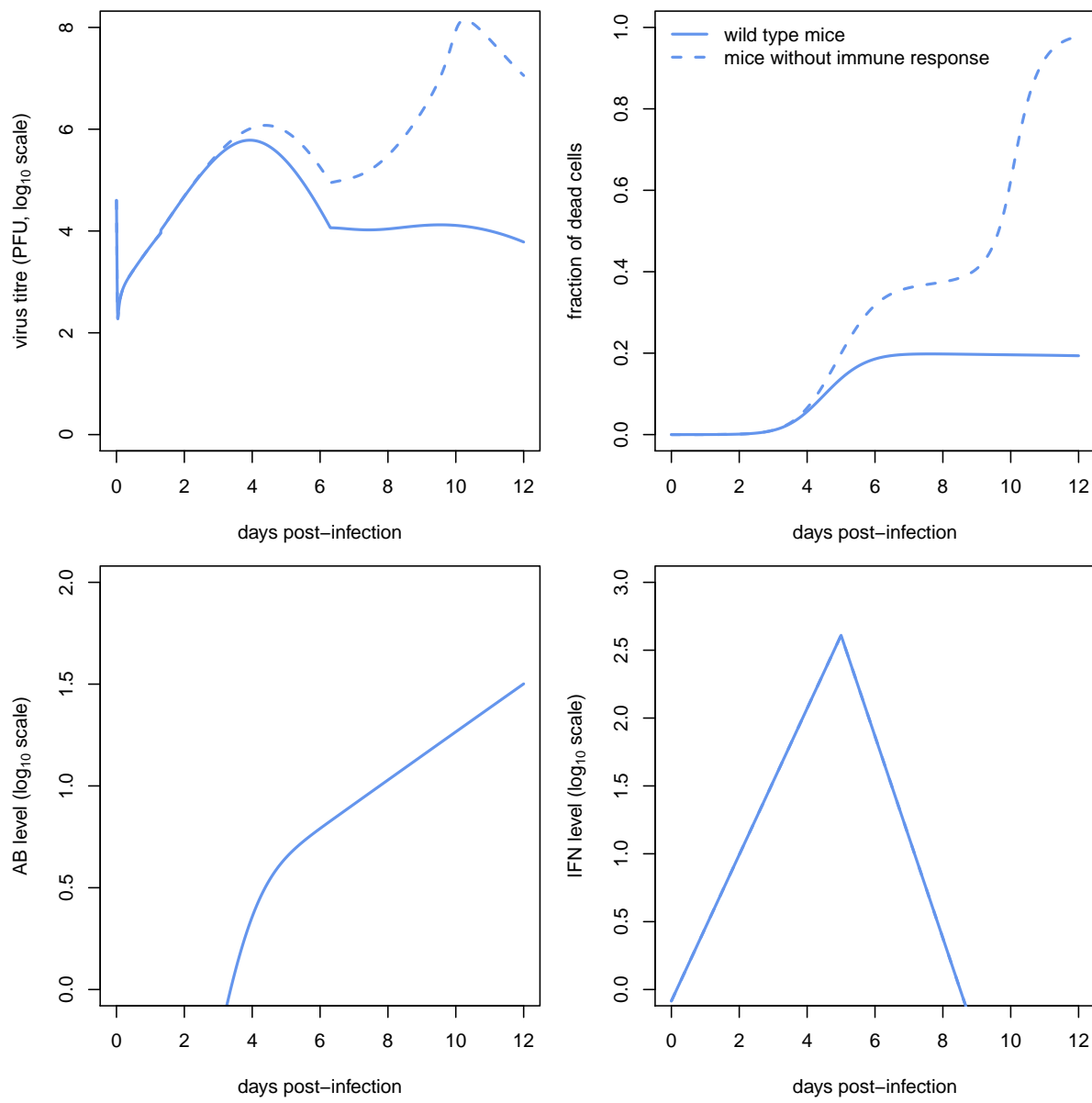


Figure S-1. Graphs reproduced using the influenza model proposed by Handel et al. [1] and described by the differential equations above. Shown in solid lines are time course for mice with functional immune system, and in dashed for mice lacking immune system.

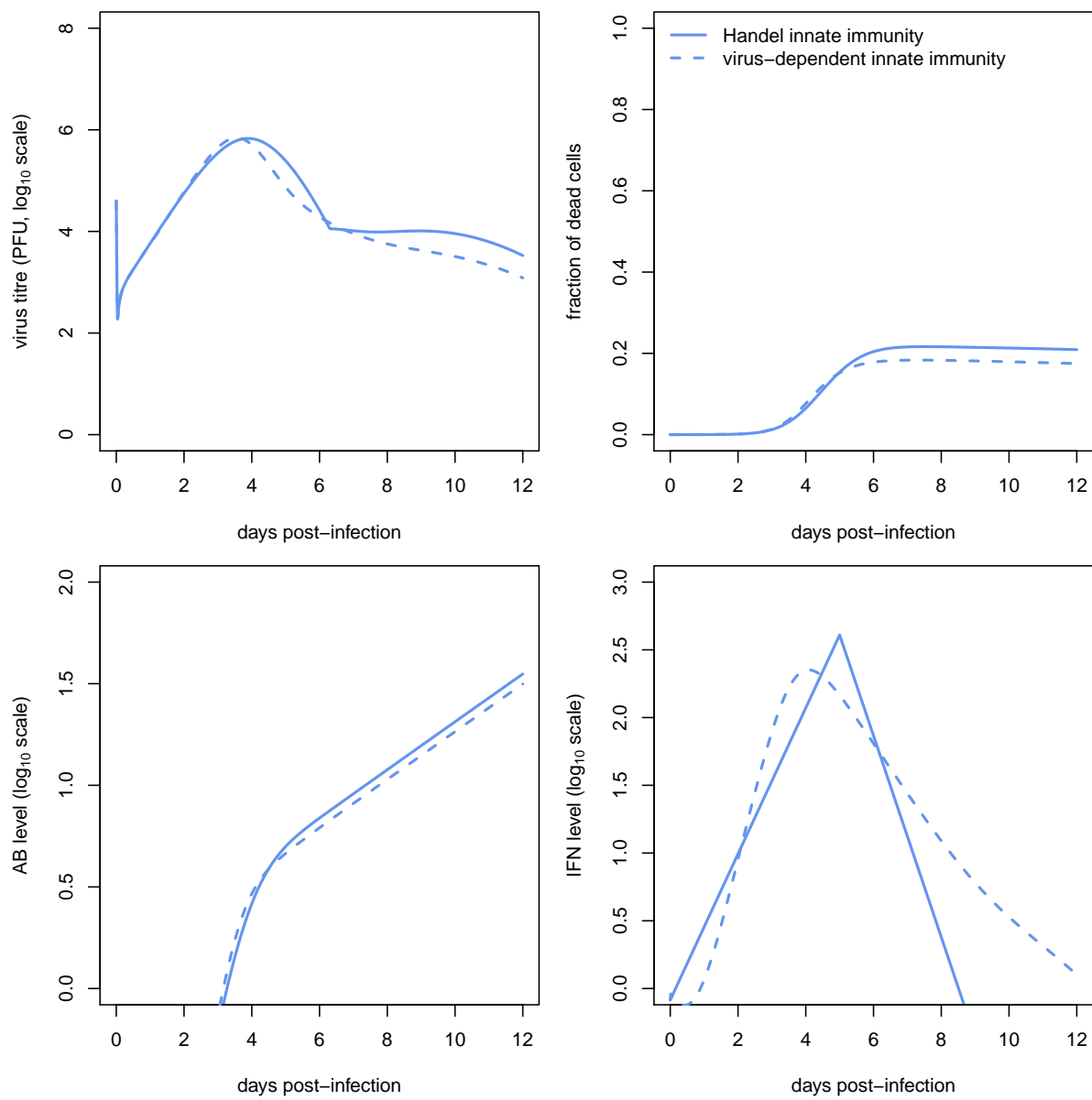


Figure S-2. The adapted model of influenza model by including virus dependent innate immunity, compared to the original influenza model proposed by Handel et al [1].

The *S. pneumoniae* model.

The mathematical model describing the within-host dynamics of pneumococcal infection is based on that proposed by Smith *et al.* [2]. The state variables are described as follows. P : pneumococci population size; T_U : uninfected cells; T_I : infected cells; C : cytokines; N : neutrophils; D : debris; and MD : derived macrophages. The system of delayed differential equations describing the time evolution of each variable is given by

$$\begin{aligned} \frac{dP}{dt} &= r P \left(1 - \frac{P}{K_P}\right) - \left[\frac{\frac{n^x M A}{P^x + n^x M A}}{1 + \kappa_D D M A} \right] \gamma_{MA} P M A - \gamma_N N P - \gamma_{MD} M D P \\ \frac{dT_U}{dt} &= -\omega P T_U \\ \frac{dT_I}{dt} &= \omega P T_U - \delta_E T_I \\ \frac{dC}{dt} &= \alpha \frac{T_I}{1 + k_N N} + \nu \frac{\theta_M P M A}{(\delta + \kappa + \theta_M P)(1 + k_N N)} - \delta_C C \\ \frac{dN}{dt} &= \eta C \left(1 - \frac{N}{N_{max}}\right) - \delta_N N - \delta_{NP} N P \\ \frac{dD}{dt} &= \rho_1 \delta_{NP} N P + \rho_2 \delta_N N + \rho_3 \delta_E T_I - \delta_D D M A \\ \frac{dMD}{dt} &= \xi N(t - \tau_P) \left(1 - \frac{M D}{M D_{max}}\right) - \delta_{MD} M D \end{aligned} \quad (\text{S-2})$$

The biological meaning and empirical estimates of parameters are provided in Table S-2¹. We refer the readers to the original paper [2] for details on the estimates. The initial conditions used to solve the system are also taken from the original paper [2], where $P(0)$ is context dependent, $T_U(0) = 1 \times 10^8$, and rest are set to 0.

¹Note that following direct correspondence with Dr. Smith, the estimates for δ_D , and k_N represented updated corrections from values presented in Smith *et al.* [2].

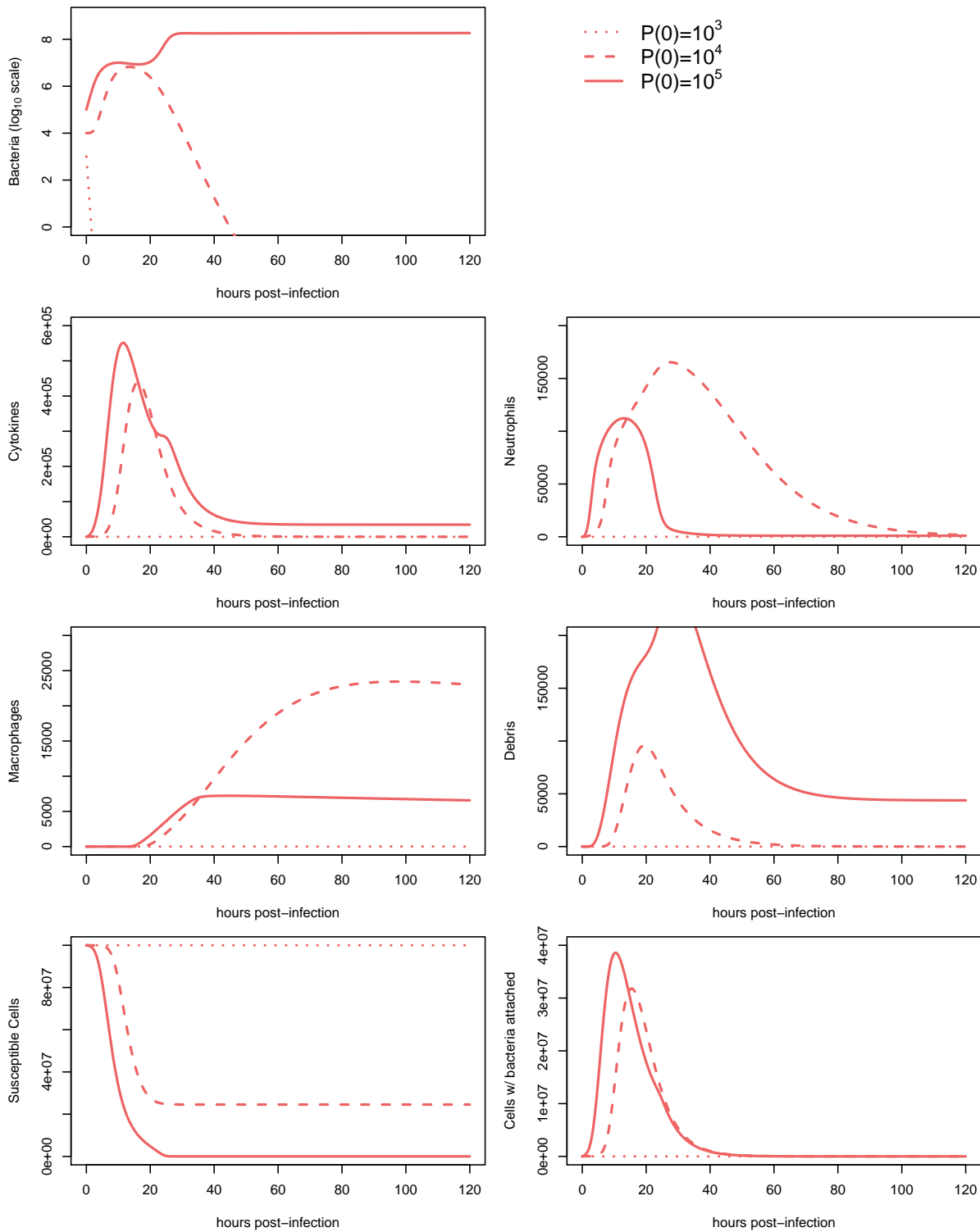


Figure S-3. Graphs reproduced using the pneumonia model [2]. Shown in solid lines are time course of the bacterial load for mice with initial inoculum of 10^5 , in dashed lines are with inoculum of 10^4 , and in dotted lines are with inoculum of 10^3 .

Table S-2. Parameters and estimates for the *S. Pneumoniae* model.

Parameter	Description	Estimate
r	bacterial growth rate	$24 \times 11.3 \times 10^{-1} \text{ day}^{-1}$
K_P	bacterial carrying capacity	$2.3 \times 10^8 \text{ CFU/ml}$
γ_{MA}	bacterial clearance by AMs	$24 \times 5.6 \times 10^{-6} \text{ per cell, day}^{-1}$
n	max. bacteria per AM	$5 \text{ CFU/ml per cell}$
x	nonlinearity	2
MA	resident alveolar macrophages	10^6 cells
γ_N	bacterial clearance by neutrophils	$24 \times 10^{-5} \text{ per cell, day}^{-1}$
θ_M	activation of cytokine production	$24 \times 4.2 \times 10^{-8} \text{ per CFU/ml, day}^{-1}$
κ	deactivation of cytokine production	$24 \times 4.2 \times 10^{-2} \text{ day}^{-1}$
ν	cytokine production by AMs	$24 \times 2.9 \times 10^{-2} \text{ pg/ml per cell, day}^{-1}$
ω	bacterial attachment to epithelial cells	$24 \times 2.1 \times 10^{-8} \text{ per CFU/ml, day}^{-1}$
δ_E	epithelial cell death	$24 \times 16.7 \times 10^{-2} \text{ day}^{-1}$
α	cytokine production by epithelial cells	$24 \times 2.1 \times 10^{-2} \text{ pg/ml per cell, day}^{-1}$
k_N	cytokine inhibition by neutrophils	$7.1 \times 10^{-6} \text{ per cell}$
δ_C	cytokine degradation rate	$24 \times 8.3 \times 10^{-1} \text{ day}^{-1}$
N_{max}	max. neutrophils	$1.8 \times 10^5 \text{ cells}$
η	neutrophil recruitment	$24 \times 13.3 \times 10^{-1} \text{ cells per pg/ml, day}^{-1}$
δ_N	neutrophil clearance rate	$24 \times 6.3 \times 10^{-2} \text{ day}^{-1}$
δ_{NP}	bacteria-induced neutrophil death	$24 \times 2.5 \times 10^{-7} \text{ per CFU/ml, day}^{-1}$
ρ_1	debris from bacteria-induced neutrophil death	10^{-1} per cell
ρ_2	debris from neutrophil death	10^{-3} per cell
ρ_3	debris from epithelial cell death	10^{-5} per cell
δ_D	removal of debris by AMs	$24 \times 10.4 \times 10^{-8} \text{ per cell, day}^{-1}$
κ_D	phagocytosis inhibition	$5.0 \times 10^{-9} \text{ per cell}$
γ_{MD}	bacterial clearance by MDMs	$24 \times 3.2 \times 10^{-5} \text{ per cell, day}^{-1}$
MD_{max}	max. MDMs	$1.8 \times 10^5 \text{ cells}$
ξ	MDM recruitment rate	$24 \times 3.8 \times 10^{-3} \text{ day}^{-1}$
δ_{MD}	MDM clearance rate	$24 \times 1.9 \times 10^{-3} \text{ day}^{-1}$
τ_P	delay in MDM recruitment	0.5 days

Influenza-Pneumococcal model

Our full model, incorporating both influenza and pneumococcal infections, is produced by coupling the single-pathogen models presented in equations (S-1) and (S-2). The key mechanism underpinning the interaction is the inhibition of alveolar macrophages via cytokines produced in the aftermath of the viral infection. The strength of the inhibition is functionally dependent on the level of innate immunity response (IR_I) elicited by the preceding viral infection, based on the findings that cytokines produced due to viral infection interferes with the functioning of the alveolar macrophages [3, 4]. The functional form, as provided in the main text, is given by the following equation

$$\Phi = 1 - \left[\frac{IR_I(t - \tau_V)}{I_{max} + K} \right]^\sigma. \quad (\text{S-3})$$

In the absence of interfering cytokines IR_I , $\Phi = 1$, and the pneumococcal infection is unaffected, and equations S-2 describe the dynamics. In the presence of cytokines IR_I , the pneumococcal model is as follows:

$$\begin{aligned}
\frac{dP}{dt} &= r P \left(1 - \frac{P}{K_P}\right) - \left[\frac{\frac{n^x \Phi MA}{P^x + n^x \Phi MA}}{1 + \kappa_D D \Phi MA} \right] \gamma_{MA} P \Phi MA - \gamma_N N P - \gamma_{MD} M D P \\
\frac{dT_U}{dt} &= -\omega P T_U \\
\frac{dT_I}{dt} &= \omega P T_U - \delta_E T_I \\
\frac{dC}{dt} &= \alpha \frac{T_I}{1 + k_N N} + \nu \frac{\theta_M P \Phi MA}{(\delta + \kappa + \theta_M P)(1 + k_N N)} - \delta_C C \\
\frac{dN}{dt} &= \eta C \left(1 - \frac{N}{N_{max}}\right) - \delta_N N - \delta_{NP} N P \\
\frac{dD}{dt} &= \rho_1 \delta_{NP} N P + \rho_2 \delta_N N + \rho_3 \delta_T T I - \delta_D D \Phi MA \\
\frac{dMD}{dt} &= \xi N(t - \tau_P) \left(1 - \frac{MD}{MD_{max}}\right) - \delta_{MD} M D
\end{aligned} \tag{S-4}$$

Antiviral treatment.

Antiviral treatment is assumed to block the production of virus by infected cells. We assume the efficacy to be 90%. Specifically, if antiviral drugs are administered at time τ_{AV} , then we model the fractional reduction of viral production as follows:

$$AV = \begin{cases} 0 & \text{if } \tau_{AV} < t \\ 0.9 & \text{if } \tau_{AV} \geq t \end{cases}$$

As a result, the influenza component of the model will have an additional term to account for the antiviral-driven reduction in viral production, which is highlighted in red below.

$$\begin{aligned} \frac{dV}{dt} &= \frac{p(1 - AV) E_I}{1 + \kappa IR_I(t - \tau_V)} - c V - \gamma b E_U V - k V IR_A \\ \frac{dIR_A}{dt} &= f V + r IR_A \\ \frac{dIR_I}{dt} &= p_1 V - p_2 IR_I \\ \frac{dE_U}{dt} &= \lambda E_D - b E_U V \\ \frac{dE_E}{dt} &= b E_U V - g E_E \\ \frac{dE_I}{dt} &= g E_E - d E_I \\ \frac{dE_D}{dt} &= d E_I - \lambda E_D \end{aligned} \tag{S-5}$$

Data from mouse experiments

Here, we discuss datasets from three mouse experiments that pertain to the prediction from the model. The first experiment, conducted by McCullers et. al. [5] explored the effect of varying the relative timing of the challenge of two pathogens, influenza virus and *S. pneumoniae*. Figure S-4[Top], shows that when *S. pneumoniae* challenge followed influenza between 3-7 days, this resulted in death of all 6 mice. The authors report that of the dying mice the ones challenged with *S. pneumoniae* 7 days post influenza lived the shortest. In contrast, in mice that were challenged with *S. pneumoniae* first, simultaneously, or more than a week later, the consequences were not as drastic. The prediction from our model showed the window of severity to be between 4-6 days. This prediction is consistent with the data in that it predicts that there is a small window of interaction spanning a few days when the interaction results in the severest forms of invasive pneumonia.

The second experiment, conducted by the same group [5], examined the dose-response to *S. pneumoniae*. Mice were first infected with influenza, and then challenged with various dose of *S. pneumoniae* at day 7—where the authors found the interaction to be the severest. Figure S-4[Bottom] shows the survival rates at various doses—even dose of 100 cfu, several orders of magnitude less than an infective dose, was sufficient to engender an infection that was severe enough to kill 50% of the mice. Such strong dose response in this window is in line with the prediction from the model.

The third experiment, conducted by McCullers [6], explored the effect of antiviral oseltamivir in mice with dual infection, when the timing of the treatment were varied. Each mouse was challenged with influenza followed by *S. pneumoniae* 7 days post influenza. Figure S-5 is reconstruction of this data, and shows that while treatment delayed by 7 days is unable to rescue any of the 6 mice, whereas the one administered after 2 days is able to treat 3 of the 6 mice. This shows that timing of the antiviral treatment is crucial. In our model, we simulated the scenario where *S. pneumoniae* followed influenza by 5 days—the timing that generated the most severe outcome in the model. With antiviral treatment, the model predicted that antiviral treatment should be administered at least 4 days post influenza to avoid this severe outcome.

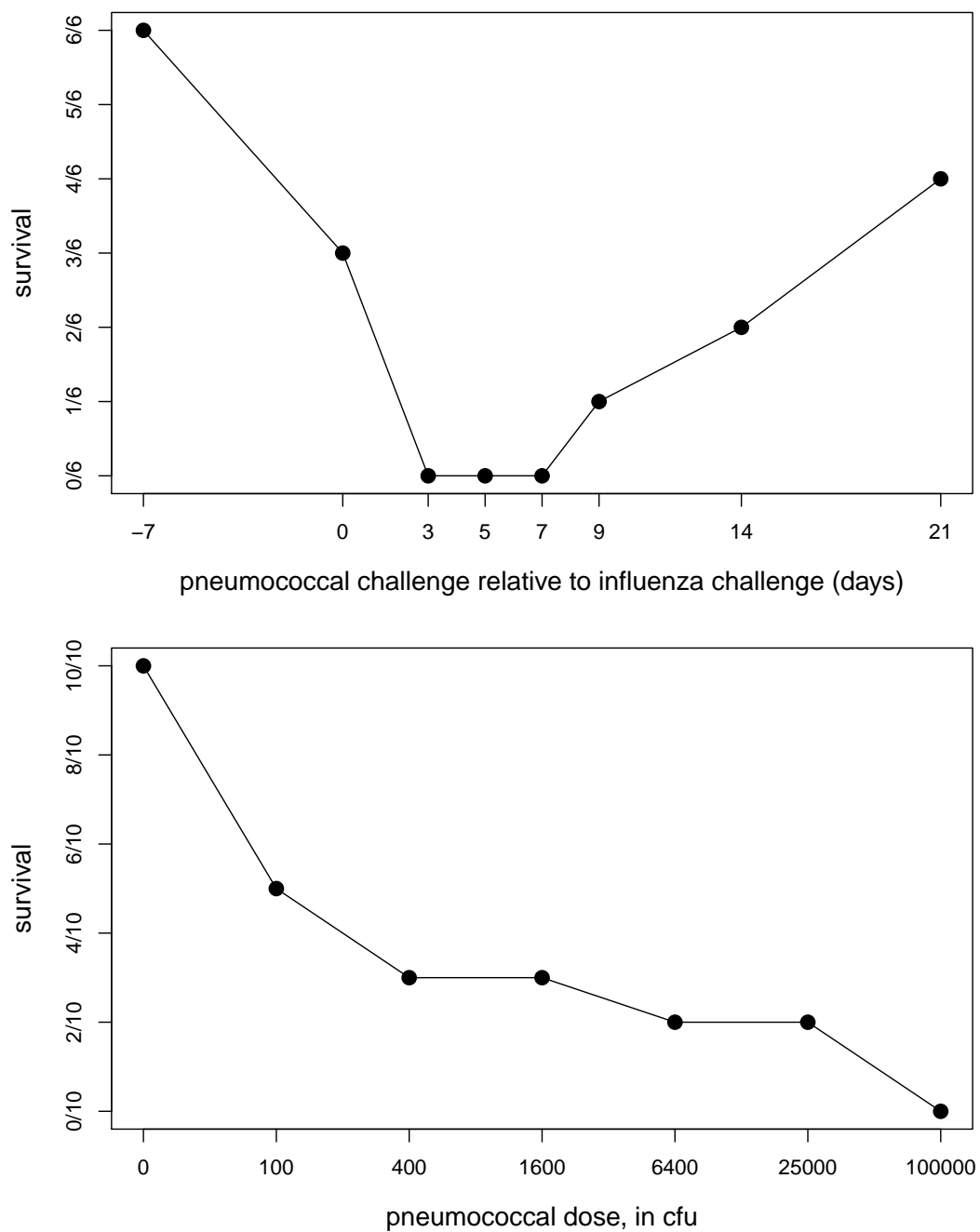


Figure S-4. [Top] Survival rates of mice challenged with both influenza virus and pneumococcus bacteria, with the relative timing shown on the horizontal axis, taken from McCullers et al, 2002 [5]. [Bottom] Survival rates of mice challenged with both influenza virus and pneumococcal bacteria, with the dose of *S. pneumoniae* varying on the horizontal axis, also taken from McCullers et al, 2002 [5]. Pneumococcal challenged followed influenza after 7 days.

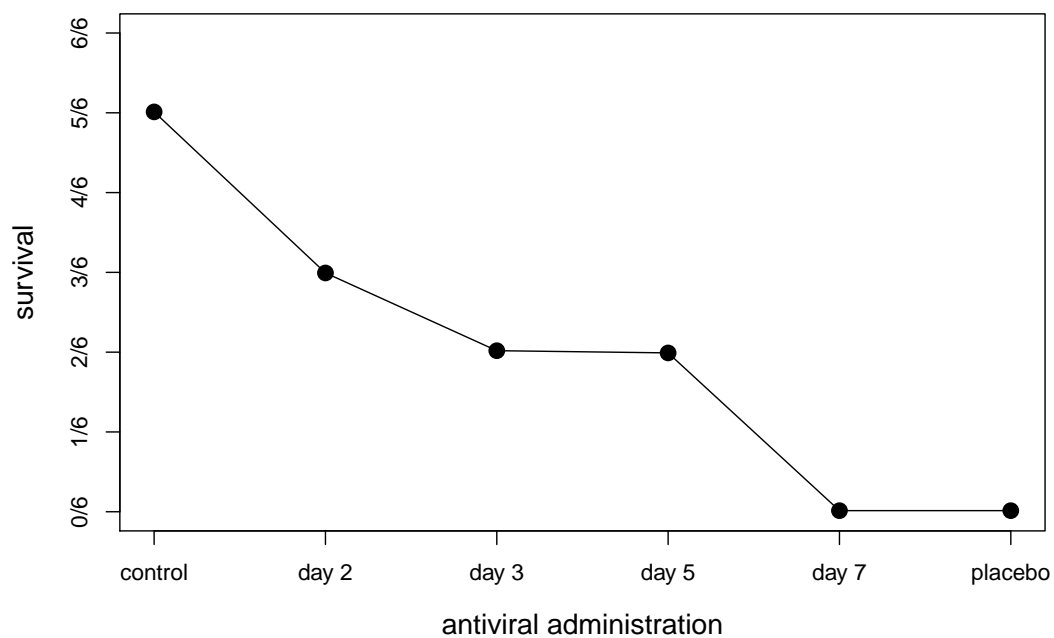


Figure S-5. Survival rates of mice challenged with both influenza virus and pneumococcal bacteria, and treated with antiviral oseltamivir beginning at different times shown on the horizontal axis, taken from McCullers, 2004 [6]. Pneumococcal challenged followed influenza after 7 days. Control mice were only challenged with *S. pneumoniae*, and placebo mice were treated with water.

Sensitivity analyses.

Sensitivity to maximal inhibition level and shape of the interference.

The model for virus-pneumococcal interaction assumes that the strength of the interaction increases linearly with interferon concentration. When the interferon levels reach a maximum, macrophages are assumed to be completely dysfunctional (This occurs when $\sigma = 1$ and $K = 0$). In Figure. S-6, we explore the effect of changing the shape (σ), as well as maximal interference (K). Decreasing the maximal interference by increasing K (moving down in the vertical direction in the figure) gradually diminishes the effect, as expected. Similarly, changing the shape of the relationship by making it saturating rather than linear (right column with exponent $\sigma = 0.5$), increases the window of enhanced susceptibility.

Sensitivity to the innate immunity model for viral infection.

Innate immunity independent of the viral production

We have used a model for innate immunity against the viral infection that depends on the viral load. The original model used by Handel *et al.* [1] assumes that viral load and innate immunity are independent. The choice of the innate immunity models slightly alters the timing of the window of enhanced susceptibility—the window is a day later in the virus-independent innate immunity model (see Figure. S-7 [C, D]).

Innate immunity dependent on infected cells

An alternative model of innate immunity, as proposed by Baccam *et al.* [7], assumes the production of innate immunity to be dependent on the infected epithelial cells. We examine the effect of such formulation. We substitute the equation for the innate immune response, IR_I , by the following:

$$\frac{dIR_I}{dt} = p_1 E_I(t - \tau_{IFN}) - p_2 IR_I.$$

τ_{IFN} was taken to be 0.5 days [7], and $p_1 = 1.5 \times 10^{-5}$, and $p_2 = 10$ —values that were picked to give approximately similar dynamics(Figure S-8).

The effect on the time and dose response remain similar, albeit the window of severity is shifted slightly to 5-7 days (see Figure S-9). The effect of antiviral treatment also remains very similar (see Figure S-10).

Sensitivity to variations of the interaction model.

Alveolar macrophages are multi-functional component of innate immunity. Apart from clearing bacteria through phagocytosis, they initiate cytokine response to recruit neutrophils and monocyte-dependent derived macrophages to aid in the further clearance of the bacteria, and clear debris formed by dead cells. In model used in the paper, we have taken the interaction to be operational on all functions of

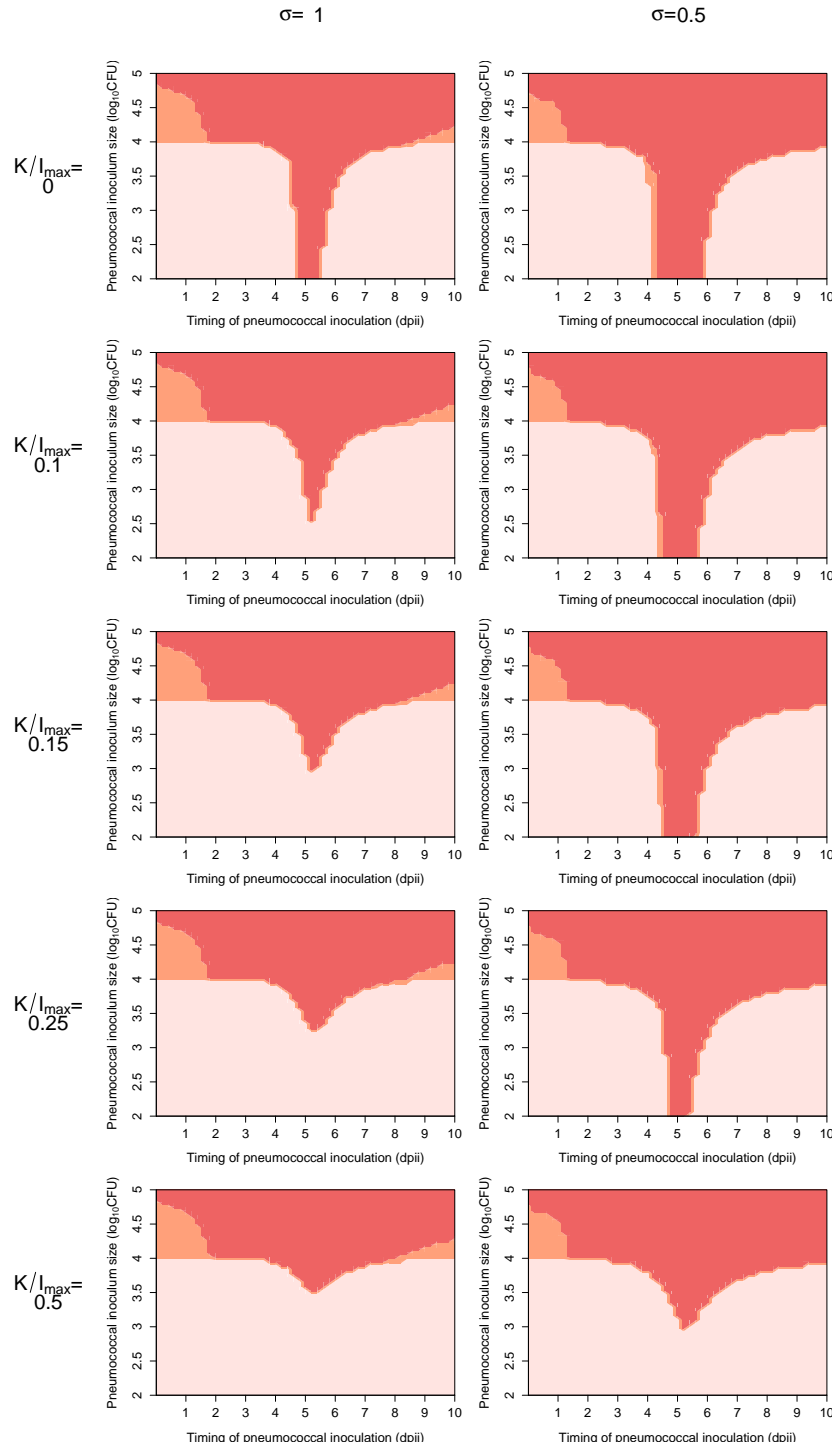


Figure S-6. Sensitivity to maximal interference level (K/I_{max} , top to bottom) and the shape of the interference (σ , left to right). For reference, the top left graph shows the results with the model used in the main paper.

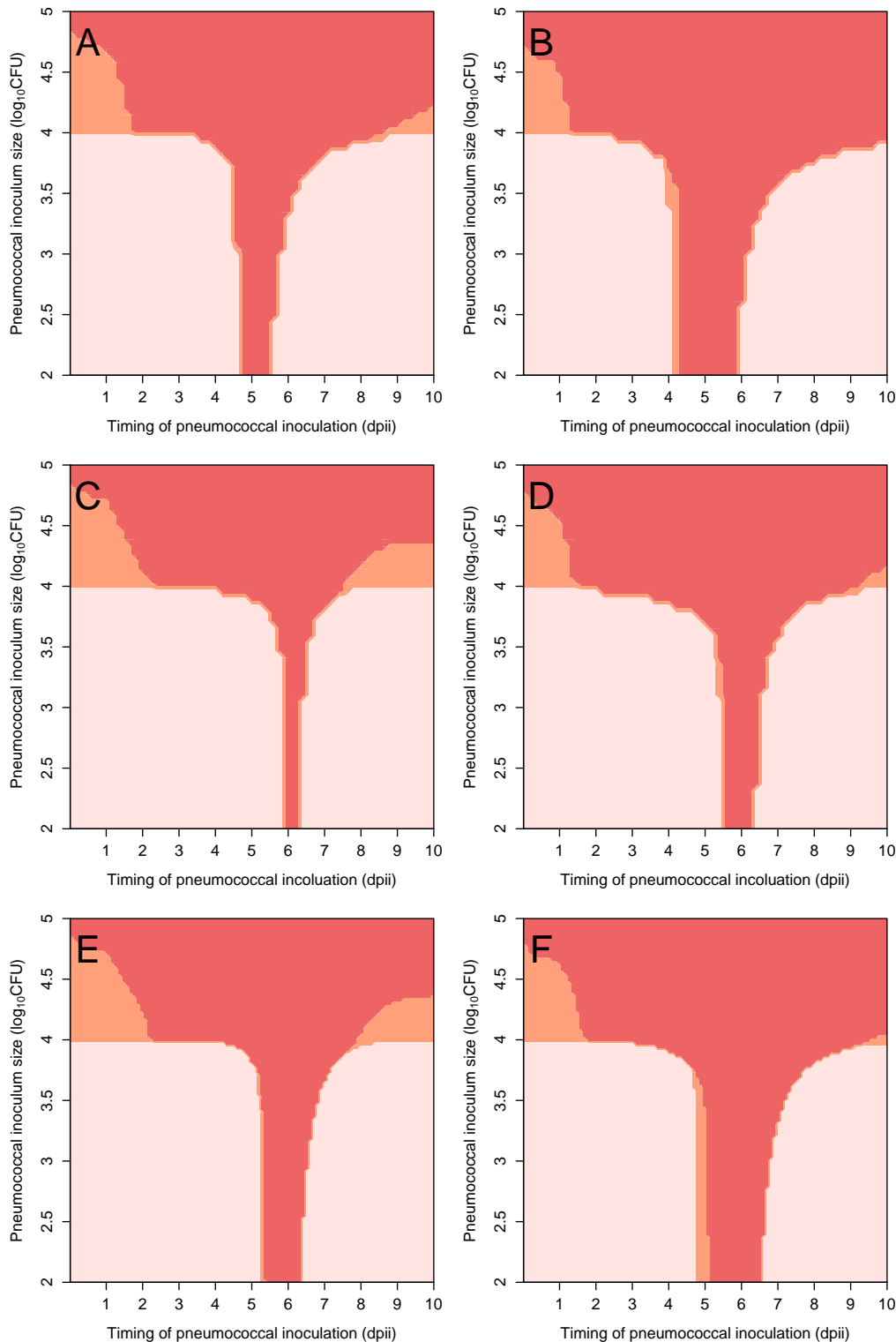


Figure S-7. Sensitivity to the innate immunity model for viral infection. The model with virus-dependent innate immunity model with [A] $\sigma = 1$ (the model used in the main text) and [B] $\sigma = 0.5$ (with saturation). The model with virus-independent innate immunity model with [C] $\sigma = 1$ and [D] $\sigma = 0.5$ (with saturation). The model with infected cell-dependent innate immunity model [7] with [E] $\sigma = 1$ and [F] $\sigma = 0.5$ (with saturation).

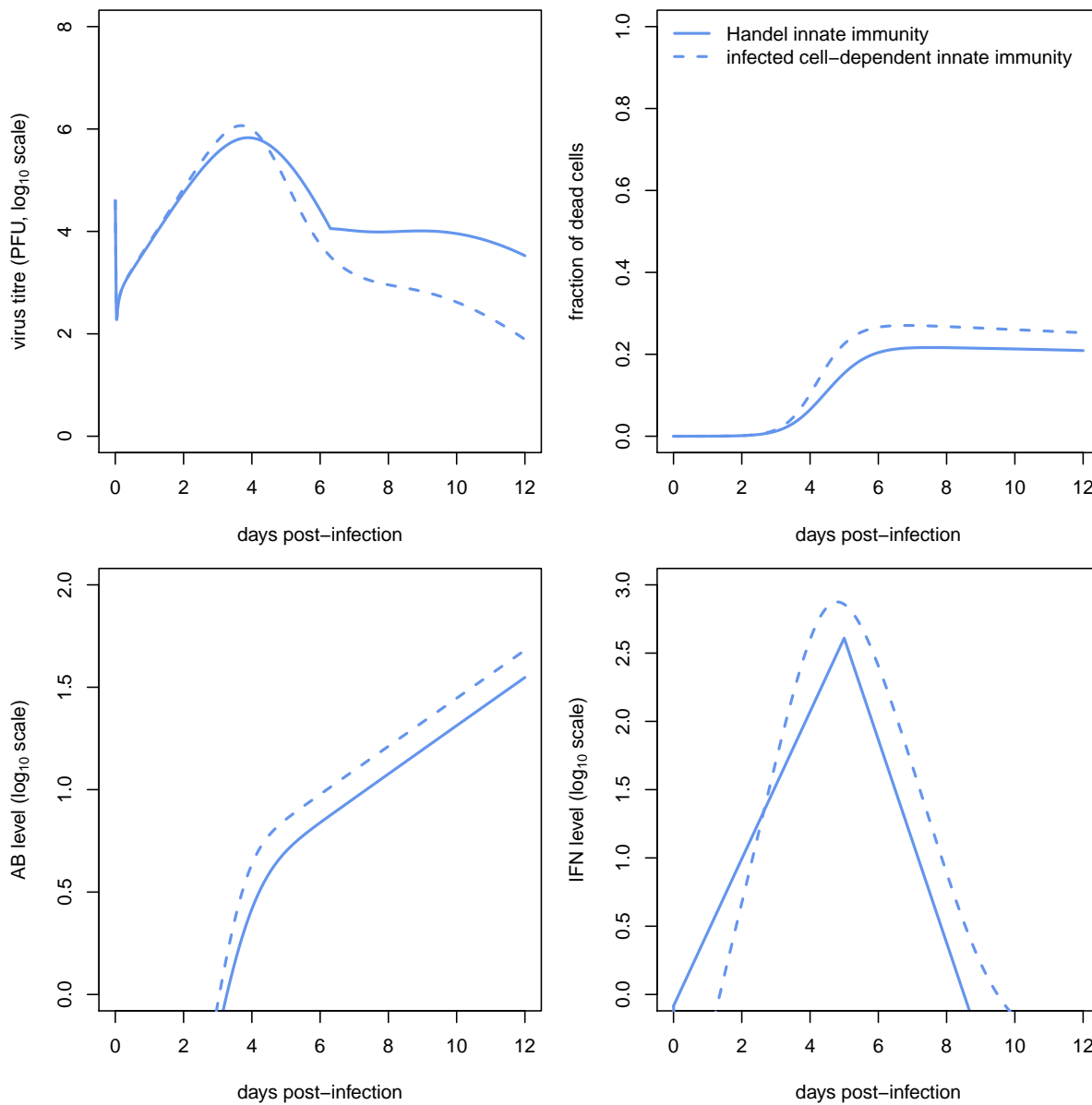


Figure S-8. Kinetics of the Handel influenza model with innate immunity modeled to depend on the infected cells [7], compared to the original influenza model proposed by Handel et al [1].

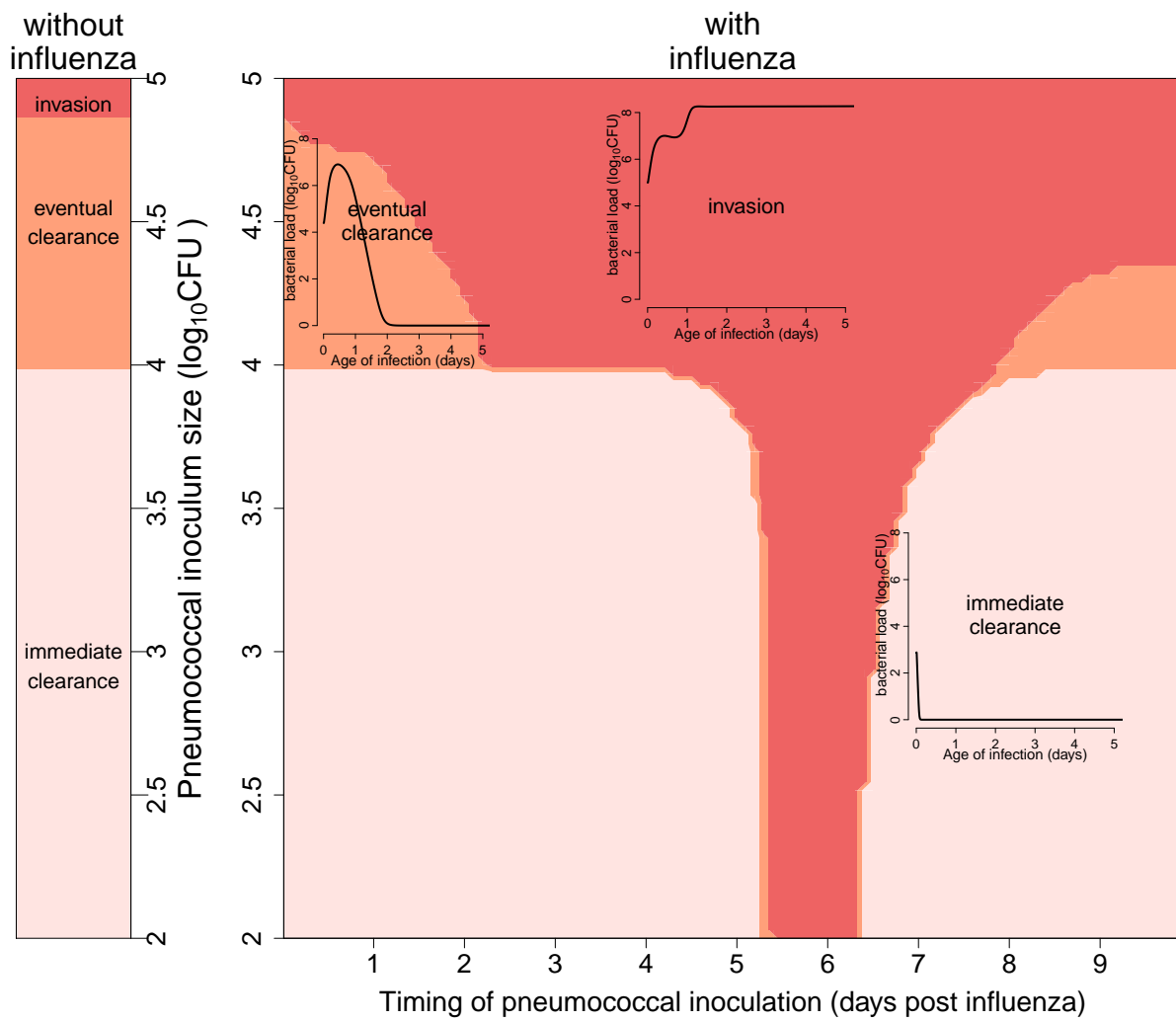


Figure S-9. Impact of interaction between influenza and pneumococcus, with innate immune response dependent on the infected cells. This figure is comparable to Figure 2 in the main text, with innate immune response dependent on the infected cells (as proposed by Baccam et al. [7]). Please read the figure legend provided for Figure 2 for details.

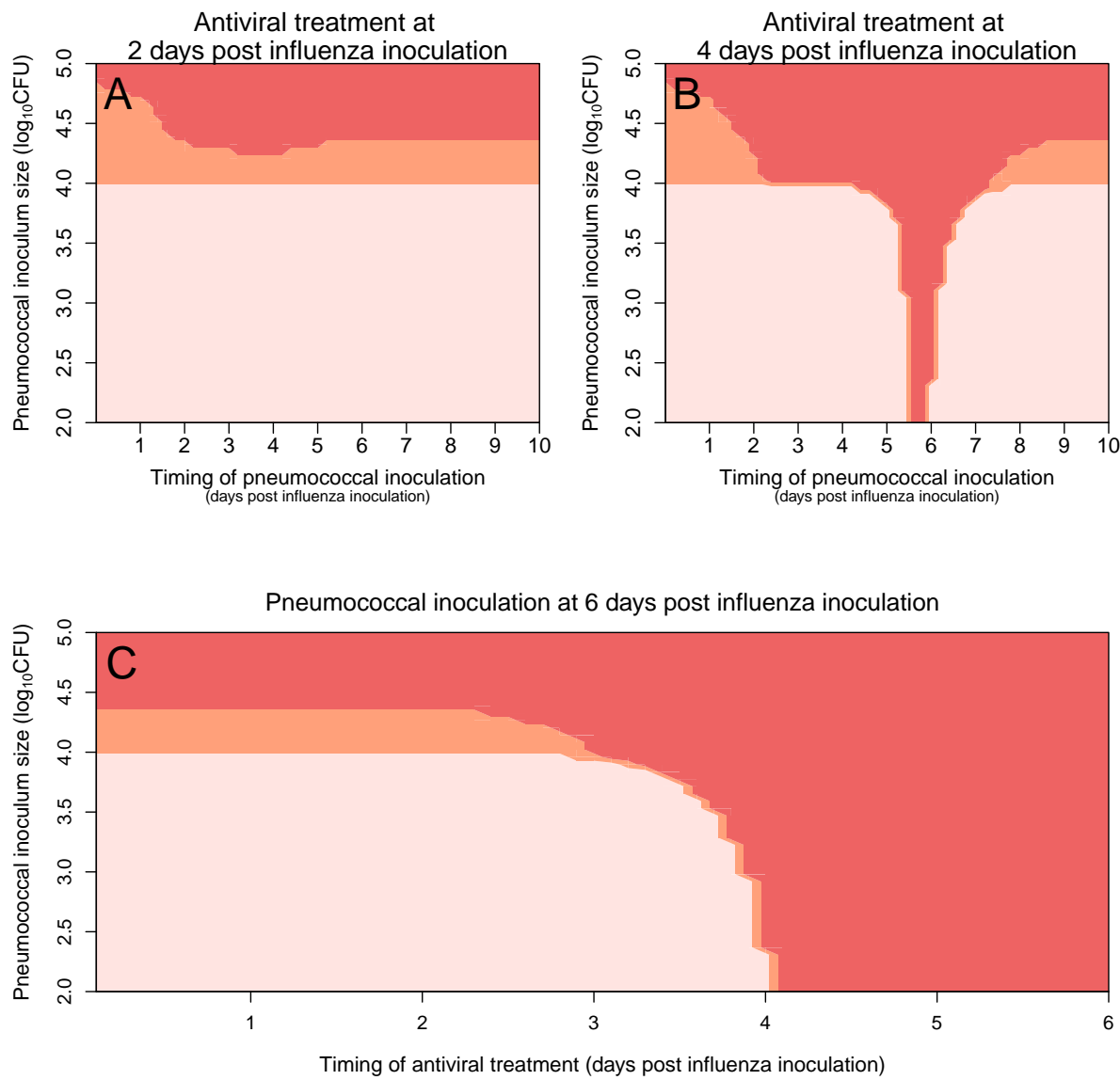


Figure S-10. Antiviral treatment in preventing severe secondary pneumococcal infection. This figure is comparable to Figure 3 in the main text, with innate immune response dependent on the infected cells (as proposed by Baccam et al. [7]). Please read the figure legend provided for Figure 3 for details.

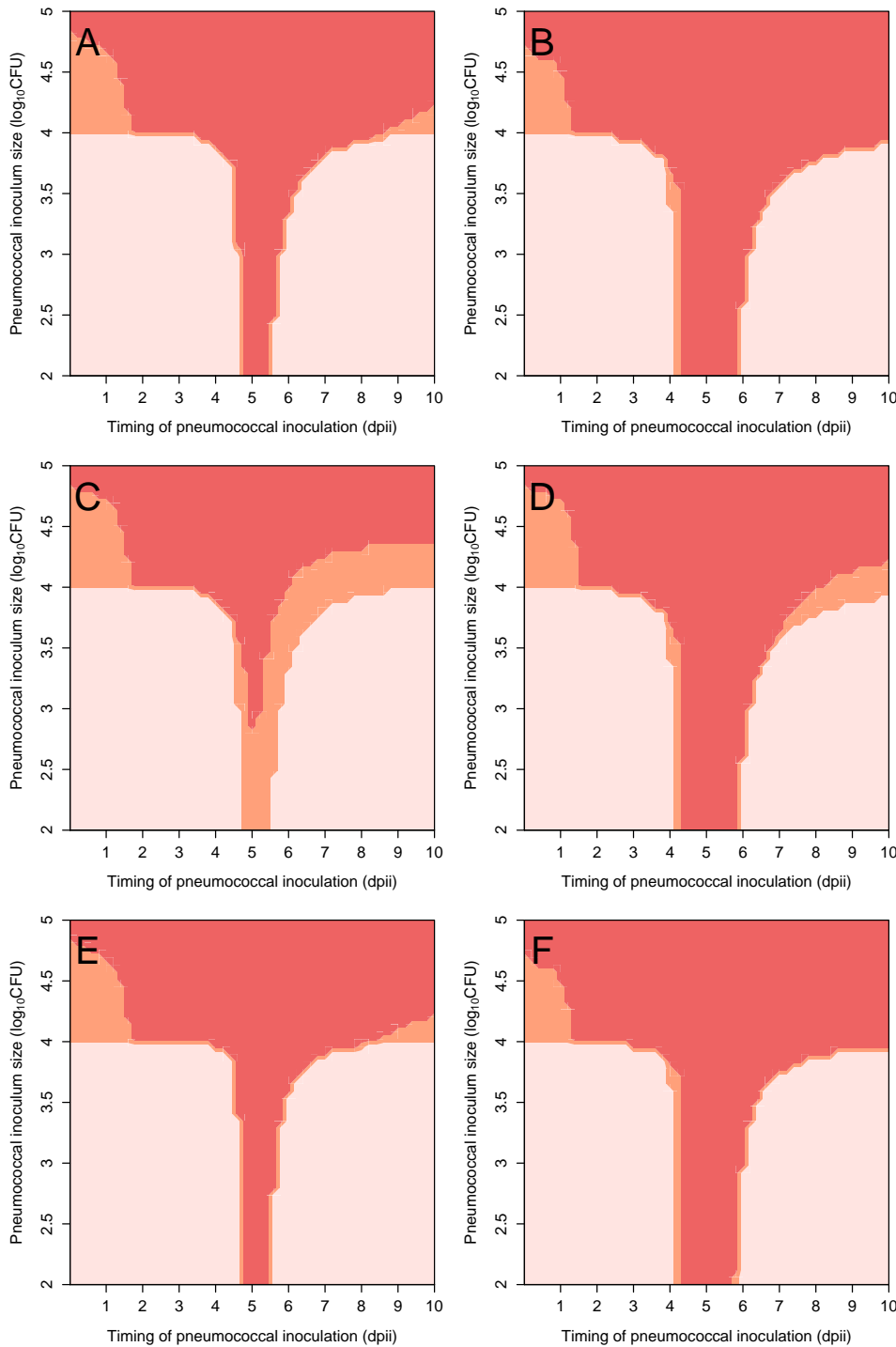


Figure S-11. Sensitivity to variations of the interaction model. [A] Interaction effect in the model used in the paper; [B] the model with saturation ($\sigma = 0.5$); [C] the effect with an interaction model that only interferes with macrophage's ability to phagocytize bacteria; [D] the model with saturation ($\sigma = 0.5$); [E] the effect when the interaction is modeled to only interfere with other functioning of macrophages excluding phagocytosis; and [F] the model with saturation ($\sigma = 0.5$).

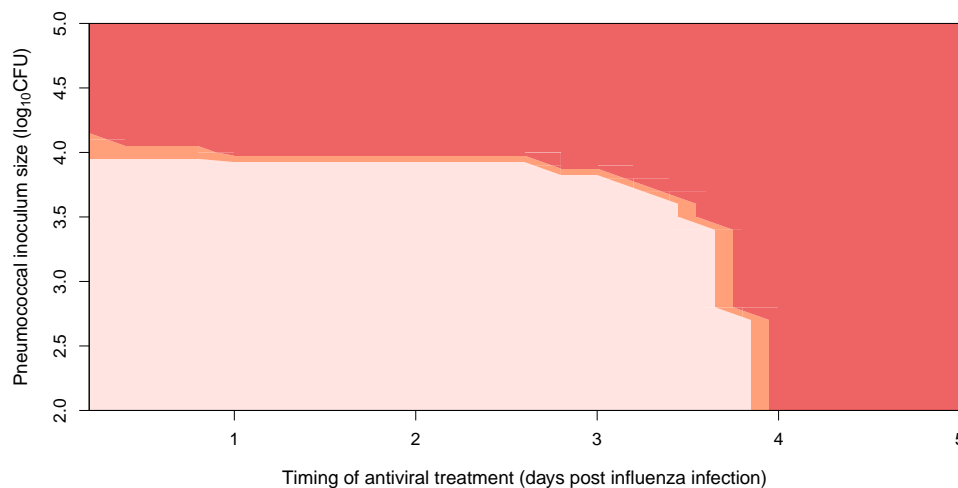


Figure S-12. Sensitivity to efficacy of antiviral treatment. The figure shows the consequences of administering treatments at various times (plotted in the horizontal axis) on the worst manifestation of the interaction (as it would at day 5 without treatment) at different intervals (plotted on the horizontal axis). The three colors represent qualitatively distinct infection outcomes: (i) severe invasive infections (dark red), (ii) acute infections that are eventually cleared (orange), and (iii) transient infections, that are cleared rapidly (pink). Compared to Fig. 3C in the main manuscript, the efficacy of the antiviral treatment here is assumed to be only 50%.

the macrophages. Here we explore the effect of the interaction is operational on specific pathways. In Figure S-11 we show that the effects are similar, either when it is only limited to the bacterial phagocytosis (Figure S-11 C,D), or it excludes phagocytosis (Figure S-11 E,F), compared to the model used in the main text (Figure S-11 A,B).

Sensitivity to efficacy of antiviral treatment.

In the main model, we assumed that the efficacy of the antiviral treatment was 90%. Here, we observe the effect of a treatment that is only 50% efficacious. Presented in Fig. S-12, are the consequences of administering treatments with only 50% efficacy. When compared to Fig. 3C in the main manuscript (90% efficacy), this figure looks mostly similar—the antiviral treatment administered before 4 days post influenza, is able to prevent severe pneumococcal infection resulting from low inocula of pneumococcus. Only difference is that the region of severe infection (red) has slightly expanded for early treatments indicating that for inocula of more than 10^4 , the antiviral treatment fail to prevent the severe outcomes of pneumococcal pneumonia. Overall, the results of antiviral treatment seems to be mostly insensitive to some variation in efficacy of the antiviral treatment. This is because, in this model, even modest reduction in the viral reproduction, particularly in the early phase, is able to prevent the viral infection from proceeding. Consequently, the model predicts that the ability to prevent severe manifestation of the interaction may be less influenced by the efficacy of the antiviral, and more by the timing of when it is administered.

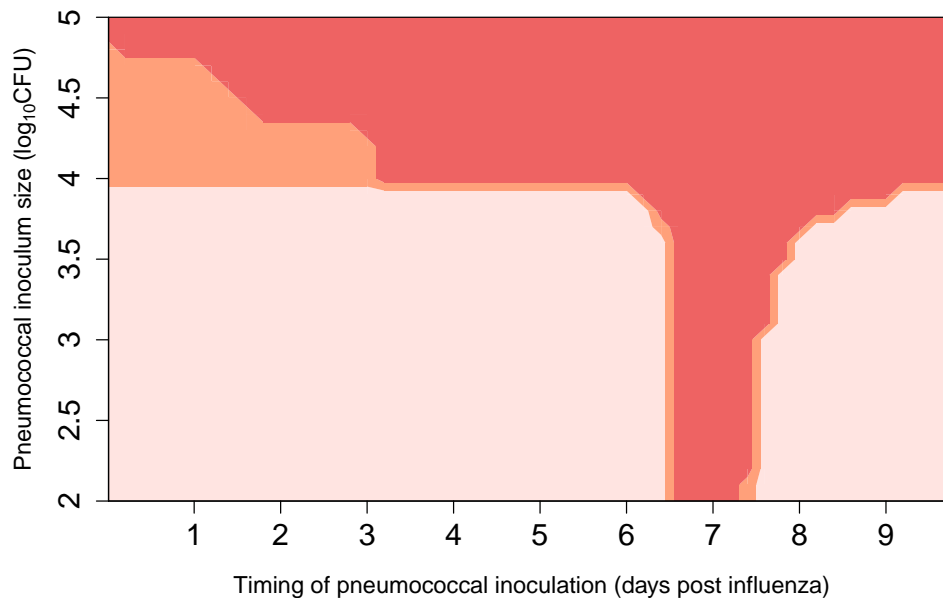


Figure S-13. Sensitivity to influenza dose response. The figure depicts the predicted clinical outcome of pneumococcal infection as a function of the timing of introduction (horizontal axis) and inoculum size (vertical axis). The three colors represent qualitatively distinct infection outcomes: (i) severe invasive infections (dark red), (ii) acute infections that are eventually cleared (orange), and (iii) transient infections, that are cleared rapidly (pink). Compared to Fig. 2 in the main manuscript, the influenza dose was reduced by two orders of magnitude to 4^2 .

Sensitivity to influenza dose response.

Influenza model [1] only explores the infection dynamics for a fixed initial dose of influenza, ie, $V(0) = 4 \times 10^4$. Here we explore the consequences of decreasing influenza dose by two orders of magnitude, $V(0) = 4 \times 10^2$. We find that in this influenza model, decreasing the influenza dose up to a certain level, delays the viral growth. This in turn delays the expression of interferon response. As a result, the window of the severe manifestation of the interaction is also pushed back (see supplementary Fig. S-13). Importantly, the severe manifestation of the interaction remains even for low dosage of influenza. This is in line with the findings by McCullers & Rehg [5], that the severe manifestation of the interaction persisted for low dosage of influenza, and decreasing the dose increased the survival times of the mice in their challenge experiments. However, we note that the influenza model was only fit for one set of data, and hence did not explicitly study the effect of dose response. Further research on influenza dose response would help elucidate the role of influenza dose response in the interaction.

References

1. Handel, A., Longini, I. & Antia, R., 2010 Towards a quantitative understanding of the within-host dynamics of influenza A infections. *Journal of The Royal Society Interface* **7**, 35–47. (doi:10.1098/rsif.2009.0067).
2. Smith, A. M., McCullers, J. A. & Adler, F. R., 2011 Mathematical model of a three-stage innate immune response to a pneumococcal lung infection. *Journal of Theoretical Biology*. **276**, 106–116. (doi:10.1016/j.jtbi.2011.01.052).
3. Sun, K. & Metzger, D. M., 2008 Inhibition of pulmonary antibacterial defense by interferon- γ during recovery from influenza infection. *Nat. Med.* **14**, 558–564. (doi:10.1038/nm1765).
4. Shahangian, A., Chow, E., Tian, X., Kang, J., Ghaffari, A., Liu, S., Belperio, J., Cheng, G. & Deng, J., 2009 Type I IFNs mediate development of postinfluenza bacterial pneumonia in mice. *J. Clin. Invest.* **119**, 1910–1920. (doi:10.1172/JCI35412).
5. McCullers, J. A. & Rehg, J. E., 2002 Lethal synergism between influenza virus and *Streptococcus pneumoniae*: Characterization of a mouse model and the role of platelet-activating factor receptor. *J. Infect. Dis.* **186**, 341–350. (doi:10.1016/j.tree.2008.05.009).
6. McCullers, J. A., 2004 Effect of antiviral treatment on the outcome of secondary bacterial pneumonia after influenza. *The Journal of Infectious Diseases* **190**, 519–526. (doi:10.1086/421525).
7. Baccam, P., Beauchemin, C., Macken, C. A., Hayden, F. G. & Perelson, A. S., 2006 Kinetics of influenza A virus infection in humans. *Journal of Virology* **80**, 7590–7599. (doi:10.1128/JVI.01623-05).